

Numerical analysis of a passively Q-switched Nd:YAG laser with a Cr⁴⁺:YAG exhibiting ESA

J. ŚWIDERSKI*, M. SKÓRCZAKOWSKI, A. ZAJĄC, and P. KONIECZNY

Institute of Optoelectronics, Military University of Technology, 2 Kaliskiego Str.,
00-908 Warsaw, Poland

Mathematical description of a passively Q-switched Nd:YAG laser has been presented. The numerical analysis of saturable absorber influence on the laser efficiency was made. The aspect taken into account here is the Cr⁴⁺:YAG – saturable absorber exhibiting excited state absorption (ESA). The optimization procedure points to the optimal circumstances of the laser system considered. The numerical model developed is a very useful tool in designing solid state lasers Q-switched by means of different nonlinear absorbers.

Keywords: Q-switched solid state laser, saturable absorber, numerical simulation.

1. Introduction

Q-switching of Nd:YAG lasers is widely applied in scientific research and for practical applications using active or passive devices. Active Q-switching methods (mechanical, electro-optic, and acousto-optic) are usually used in Nd:YAG systems to obtain pulses with high repetition rate and high average output power [1]. The technique of active Q-switching is rather complicated but the advantage is the fact that the repetition rate is independent of pumping power. The alternative technique of laser losses switching is application of a saturable absorber whose transmission depends on internal laser flux intensity. In this technique, a material with high absorption at the laser wavelength is placed inside the laser resonator and prevents laser oscillation until the population inversion reaches a value exceeding the total optical losses (dissipative losses, saturable absorber losses, transmission losses) inside the laser cavity. As the photon density builds up following achievement of a net positive inversion, passive absorber rapidly bleaches into a high transmission state, thereby Q-switching the laser.

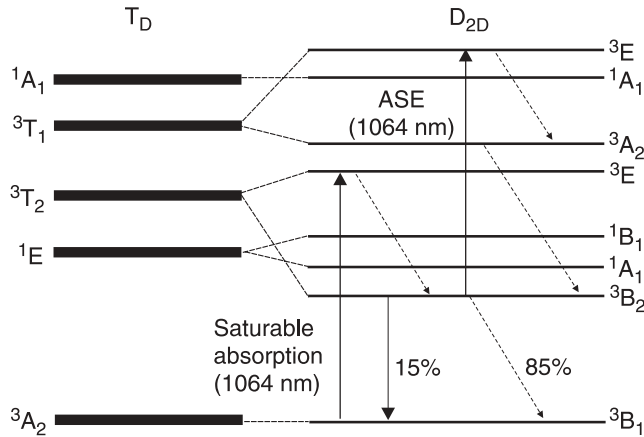
There are some advantages and disadvantages of both passive and active Q-switches. By using an active Q-switch, the repetition rate can be controlled by an external driver, whereas for a passive Q-switch the repetition rate is given by the internal parameters of the laser. The passive Q-switch is initiated by the laser intensity inside the resonator itself. Therefore, this Q-switch is simple – there is no need for drivers but, at the same time, the flexibility in choosing laser parameters is reduced. This means it is not possible to change the repetition rate for a given input pumping power and absorber transmission. At high

depth of modulation, the residual losses are also high and therefore the efficiency is low. Other disadvantages of the passive Q-switch are: the large build-up of time fluctuations and the intensity instability from pulse to pulse. However, compared with active Q-switching methods, passive techniques that use saturable absorbers can significantly simplify the operation and alignment, improve the reliability and compactness, and reduce the costs of laser sources.

2. Short characteristics of Cr⁴⁺:YAG crystal

Recently, a Cr⁴⁺:YAG as a Q-switched elements used for Nd:host lasers have attracted great attention [2,3]. The energy level diagram of Cr⁴⁺:YAG crystal is shown in Fig. 1. As it is shown in Fig. 1, a four-level model can explain the saturable effects at 1064-nm wavelength. The ¹E level splits in ¹A₁ and ¹B₁. The absorption of the radiation at 1064 nm occurs between the level ³E(³T₂) and the ground level. The excited level decays by photon interaction to the level ³B₂(³T₂), which relaxes by spontaneous emission. The quantum efficiency of the transition ³B₂ → ³B₁ is poor (15%) at room temperature and decreases with temperature increase. The strong photon interaction is responsible for a small value of the quantum efficiency. The energy balance at 1064 nm is as follows: from 9400 cm⁻¹ a part of 2600 cm⁻¹ is transformed into heat by photon interaction ³E → ³B₂, 85% of the rest (6800 cm⁻¹) is transformed into heat because of the low quantum efficiency. The excited state absorption (ESA) phenomenon appears between the ³B₂ and ³E (³T₁) levels. Relaxation of the ³E (³T₁) level is supposed to be reduced entirely through photon interaction. The transition ³A₂ → ³E (³T₂) has the cross section of 1.5×10⁻¹⁸ cm² and the transition ³B₂ (³T₂) → ³E (³T₁) has the cross section of 1×10⁻¹⁹ cm².

* e-mail: jswiderski@wat.edu.pl


 Fig. 1. Energy level diagram of a Cr⁴⁺:YAG crystal.

Cr⁴⁺:YAG crystal is superior to the traditional Q-switched saturable absorbers (Kodak dyes, celluloseacetate thin films or LiF:F₂ crystals, etc.) for such reasons as: its excellent optical properties, large absorption cross section, high damage threshold and no degradation. Therefore it is reasonable to believe that Cr⁴⁺:YAG is an ideal saturable absorber as a passive Q-switch for all high power and high repetition rate solid state lasers.

3. Rate equations for passively Q-switched Nd:YAG lasers

Passive Q-switching is currently the most attractive method of generation of ns and sub-ns laser pulses. The main characteristics of a Q-switch are as follows: the concentration of absorption centers, ground state absorption (GSA), excited state absorption (ESA) cross sections, and lifetimes of the upper levels. To design the passively Q-switched laser properly, we should know all these parameters as well as the potential gain in the lasing medium (LM) and its scatter losses. There are some works [4,5] where the problem of design and optimization of passively Q-switched lasers with saturable absorbers (SA) exhibiting ESA was solved. However, in these works, the solutions were limited to the case of the so-called “slow absorber”. In this paper we developed a detailed analysis of passively Q-switched lasers based on the normalized dimensionless rate equations taking into account: ESA and lifetimes of SA levels as well as the magnification in the laser cavity.

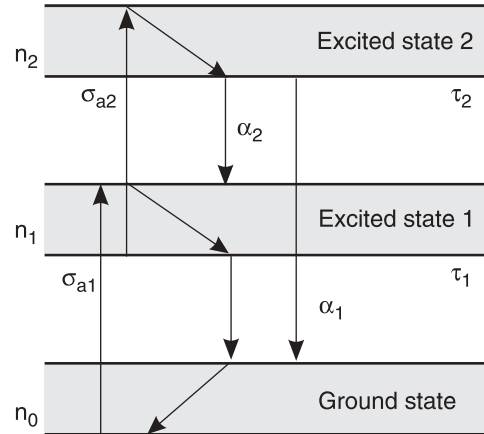


Fig. 2. Energy level diagram of a saturable absorber characterized by ESA.

The situation where a saturable absorber is characterized by only one excited state seldom occurs in nature. In reality, a saturable absorber is usually characterized by more than one excited state to which molecules from ground state are transported. The molecules, which are located in excited state, can be transported even to the higher excited levels (on the condition that the energy gap of adjacent excited levels equals the energy of absorption quantum). This situation is depicted in Fig. 2. The parameters marked in this figure are as follows: n_0, n_1, n_2 is the population density of the ground state, the first and the second excited state, respectively, σ_{a1} is the absorption cross section from the ground state to the first excited state of SA, σ_{a2} is the absorption cross section from the first to the second excited state of SA, τ_1, τ_2 is the lifetime of the first and the second excited state, respectively, α_1, α_2 is the deactivation coefficient of SA centers from the second to the first excited state and to the ground state (the sum of α_1 and α_2 equals one, $\alpha_1 \ll \alpha_2$).

According to literature reports, there are many saturable absorbers, in which excited state absorption phenomenon occurs. The most common are dielectrics doped with different active ions, like chromium, vanadium, erbium, cobalt, thulium and many others [6–9].

A passive Q-switched laser system with saturable absorber characterized by ESA can be described by four rate equations relating to average power density in the laser cavity J , amplification in the laser medium k , the population density of the first n_1 and the second n_2 excited state

$$\frac{dJ(t)}{dt} = V_R \left\{ k(t) - \rho_s - \frac{l_{SA}}{l_{LM}} \sigma_{a1} \left[N_0 - n_1(t) - n_2(t) + \frac{\sigma_{a2}}{\sigma_{a1}} n_1(t) \right] \right\} J(t), \quad (1)$$

$$\frac{dk(t)}{dt} = \bar{\omega}_p [\chi - k(t)] - \frac{k(t)}{\tau_{LM}} - \frac{k(t)J(t)}{Es}, \quad (2)$$

$$\frac{dn_1(t)}{dt} = M^2 \frac{J(t)}{Es_{a1}} \left\{ [N_0 - n_1(t) - n_2(t)] - \frac{\sigma_{a2}}{\sigma_{a1}} n_1(t) \right\} - \frac{n_1(t)}{\tau_1} + \frac{\alpha_2 n_2(t)}{\tau_2}, \quad (3)$$

$$\frac{dn_2(t)}{dt} = M^2 \frac{J(t)}{Es_{a2}} n_1(t) - \frac{n_2(t)}{\tau_2}, \quad (4)$$

with the initial conditions

$$k(t=0) = k_0, \quad (5)$$

$$J(t=0) = J_0, \quad (6)$$

where $Es_{a1} = h\nu_s/\sigma_{a1}$ is the saturation energy of the nonlinear absorber to the first excited state, $Es_{a2} = h\nu_s/\sigma_{a2}$ is the saturation energy of the nonlinear absorber to the second excited state, $Es = h\nu_s/\sigma_e$ is the saturation energy of the laser medium (the energy that can be stored in LM), $N_0 = n_0 + n_1 + n_2$ is the total population density of SA absorbing centers, $h\nu_s$ is the photon energy, ω_p is the pumping speed of the active medium, M is the enlargement of an internal beam in a laser cavity (the ratio of cross-sectional area of a beam in SA to cross-sectional area of a beam in LM), l_{LM} and l_{SA} are the lengths of LM and SA, respectively, χ is the theoretical maximum gain which can be obtained in LM ($\chi = n_0\sigma_e$), σ_e is the emission cross-section of LM, $V_R = c(l_{LM}/L_{opt})$ is the speed of light in the resonator, τ_{LM} is the fluorescence lifetime of LM, ρ_s is the static losses coefficient which includes the dissipative ρ_d and the transmission ρ_t losses, and L_{opt} is the optical length of the resonator.

To describe the Q-switched laser, we used a point model. This model is good enough for passive Q-switching. The analysis and solution of the rate equations presented above allow us to depict the dynamics of laser generation in the system discussed.

4. Normalized rate equations for passively Q-switched Nd:YAG lasers

The mathematical description of a passively Q-switched solid-state laser, given in the prior section, includes functions and parameters whose values are dimensional and absolute. It makes more detailed physical interpretation of these equations difficult and permits to solve them only for specific cases. Obtaining the quantitative information, typical for analytical solution of the problem discussed, is impossible in this case. Therefore the rate Eqs. (1)–(4) should be transformed into a form in which their functions and parameters will have relative values, linked with certain material constants or laser system features. It guarantees to formulate more general conclusions related to a laser with a saturable absorber as a passive switch and enables its optimization.

In the analysis proposed, the laser energy balance was taken into account. Depending on $M^2\delta_1$ parameter, being normalized pumping speed of a saturable absorber, the changes of energy generated in a laser with its division between energy emitted on static and dynamic losses were examined. The initial gain and different relations of static and dynamic losses in a laser cavity were changeable.

In connection with foregoing, the following normalized and dimensionless quantities are introduced (Table 1).

Table 1. Definitions of normalized constants and variables.

Constant	Symbol	Definition
Normalized power density in the laser cavity	I	$\frac{JL_{opt}}{Esc}$
Normalized gain of LM	K	$\frac{k}{\chi}$
Normalized population of the first excited state of SA	N ₁	$\frac{n_1}{N_0}$
Normalized population of the second excited state of SA	N ₂	$\frac{n_2}{N_0}$
Normalized fluorescence lifetime of LM	T _{LM}	$\frac{\tau_{LM}c}{L_{opt}}$
Normalized lifetime of the first excited state of SA	T ₁	$\frac{\tau_1c}{L_{opt}}$
Normalized lifetime of the second excited state of SA	T ₂	$\frac{\tau_2c}{L_{opt}}$
Normalized pumping speed of LM	W _p	$\frac{\omega_p L_{opt}}{c}$
Normalized static losses of the laser cavity	R _s	$\frac{\rho_s}{\chi}$
Normalized initial dynamic losses of the laser cavity related to SA	Γ _{SA}	$\frac{\gamma_{SA}}{\chi}$
Normalized transmission losses of the laser cavity	R _T	$\frac{\rho_t}{\chi}$
Normalized dissipative losses of the laser cavity	R _D	$\frac{\rho_d}{\chi}$

Introduction of the constants defined in Table 1 modifies Eqs. (1)–(4) to the following form

$$\frac{dI}{dT} = l_{LM}\chi\{K - R_s - \Gamma_{SA}[(1 - N_1 - N_2) + \delta N_1]\}I, \quad (7)$$

$$\frac{dK}{dT} = W_p(1 - K) - \frac{K}{T_{LM}} - KI, \quad (8)$$

$$\frac{dN_1}{dT} = M^2 I \delta_1 [(1 - N_1 - N_2) - \delta N_1] - \frac{N_1}{T_1} + \frac{\alpha N_2}{T_2}, \quad (9)$$

$$\frac{dN_2}{dT} = M^2 I \delta_1 \delta N_1 - \frac{N_2}{T_2}, \quad (10)$$

with the initial conditions

$$I(0) = \frac{\chi l_{LM}}{T_{LM}} (R_s + \Gamma_{SA}) \frac{\Omega}{4\pi}, \quad (11)$$

$$K_{OA}(0) = R_s + \Gamma_{NA}, \quad (12)$$

$$N_1(0) = 0, \quad (13)$$

$$N_2(0) = 0, \quad (14)$$

where

$$\delta = \frac{\sigma_{a2}}{\sigma_{a1}}, \quad (15)$$

$$\delta_1 = \frac{\sigma_{a1}}{\sigma_e}, \quad (16)$$

$$\gamma_{SA} = \frac{l_{SA} N_0 \sigma_{a1}}{l_{LM}}, \quad (17)$$

Ω is the solid angle of laser generation.

Using the rate Eqs. (7)–(10) we can find an expression describing the values of energy in a laser with a saturable absorber. It can be output energy, energy scattered on static, dynamic losses of a laser cavity or energy stored in a laser medium.

As it results from the principle of operation of the laser considered, during its pumping process, the energy is stored in it as long as the gain reaches the static losses and initial dynamic losses delivered by a saturable absorber. After the generation threshold overflow, the gain in LM increases due to still working pump, however, this increase is usually insignificant. Therefore it can be assumed that energy stored in a laser medium corresponds to the state where the gain equals the initial cavity losses. Hence, the energy stored in 1 cm² of LM cross section surface can be given by

$$E_{stored} = kEl_{LM}. \quad (18)$$

Linking this expression with saturation energy of LM we receive the normalized stored energy

$$E_{stored}^N = \frac{E_{stored}}{E_s} = \chi_{LM}^l (R_s + \Gamma_{SA}). \quad (19)$$

After crossing the generation threshold in LM ($T = 0$), the lasing begins and continues until the laser medium saturates ($T = T_k$). The power generated is distributed on static and dynamic losses and can be described by

$$E_{STAT} = \rho_s l_{LM} \int_0^{t_k} J dt, \quad (20)$$

$$E_{DYN} = l_{LM} \int_0^{t_k} J(t) \rho_D(t) dt. \quad (21)$$

Integrating and linking these expressions with saturation energy of an active medium we receive the normalized energy, emitting on static and dynamic losses of a laser cavity

$$E_{STAT}^N = \frac{E_{STAT}}{E_s} = R_s \chi_{LM}^l \int_0^{T_k} IdT, \quad (22)$$

$$E_{DYN}^N = \frac{E_{DYN}}{E_s} = \Gamma \chi_{SA}^l l_{LM} \int_0^{T_k} I(1 - N_1 + \delta N_1 - N_2) dT. \quad (23)$$

The normalized output energy is given by

$$E_{out}^N = \frac{E_{out}}{E_s} = R_T \chi_{LM}^l \int_0^{T_k} IdT. \quad (24)$$

Normalized Eqs. (7)–(10) are the nonlinear system of equations and they do not have trivial analytical solutions. Thus, they were solved by means of numerical methods.

5. Numerical analysis results

The whole analysis was conducted in two aspects. In $M^2\delta_1$ parameter domain, we searched for the situation where the energy necessary to switch dynamic losses would be possibly small while the energy emitted on static losses would be the highest. However, in dynamic to static losses ratio domain, we searched for the situation when the output energy of the laser would be maximum. To this end, Eqs. (7)–(10) were integrated and then suitable integrals occurring in Eqs. (22)–(24) were calculated.

All the calculations were conducted for the following data: $\chi_{LM}^l = 300$, $W_p = 10^{-7}$, $T_{LM} = 10^4$, $R_s + \Gamma_{SA} = 0.01$. Participation of the dynamic losses Γ_{SA} in the laser cavity was variable and equaled 90%, 80%, and 70% of the whole value of initial LM losses. The value of $M^2\delta_1$ parameter was variable in the range from 0 to 100. The normalized lifetimes of SA excited states equaled: $T_1 = 1000$ or 1 and $T_2 = 1$.

Figures 3 and 5 depict the dependence of energy emitted on static (dissipative and transmission) losses as a function of $M^2\delta_1$ for high initial gain and for two different values of T_1 time. As you can see, E_{STAT}^N always rises along with the increase of $M^2\delta_1$ value. The most explicit changes occur in the range of intermediate values of $M^2\delta_1$, where the highest changes of E_{STAT}^N occur. The high value of $M^2\delta_1$ accompanies the insignificant increment of E_{STAT}^N . These relations depend on Γ/R_s ratio only to a minimum extent.

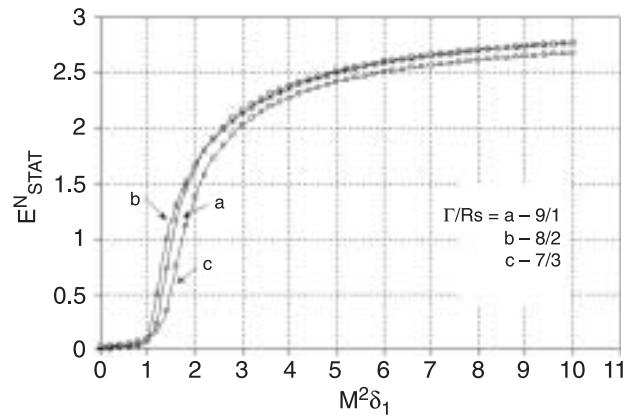


Fig. 3. Normalized energy emitted on static losses of the laser cavity vs. $M^2\delta_1$ parameter for SA without ESA. $T_1 = 1000$.

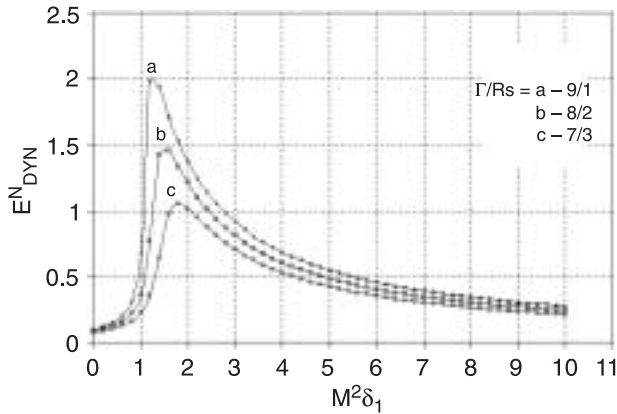


Fig. 4. Normalized energy emitted on dynamic losses of the laser cavity vs. $M^2\delta_1$ parameter for SA without ESA. $T_1 = 1000$.

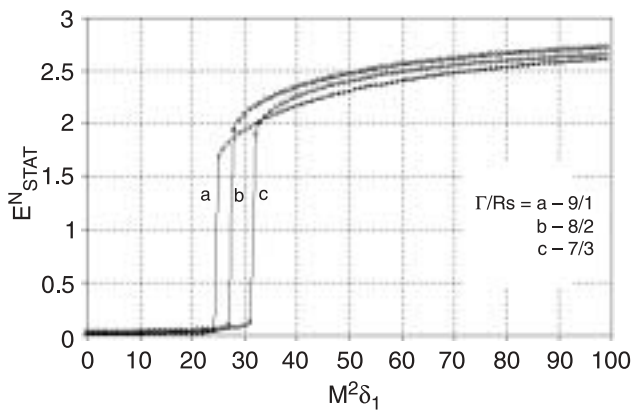


Fig. 5. Normalized energy emitted on static losses of the laser cavity vs. $M^2\delta_1$ parameter for SA without ESA. $T_1 = 1$.

In Figs. 4 and 6, the dependence of the energy emitted on dynamic losses versus $M^2\delta_1$ parameter was presented. What we can quantitatively determine from this diagram is the energy which is necessary to saturate the SA – as far as effective laser losses switching is concerned, this range is the most relevant. Along with the increase of Γ/R_s ratio, the maximum of E_{DYN}^N shifts towards the lowest values of $M^2\delta_1$ and the value of this maximum decreases. It deter-

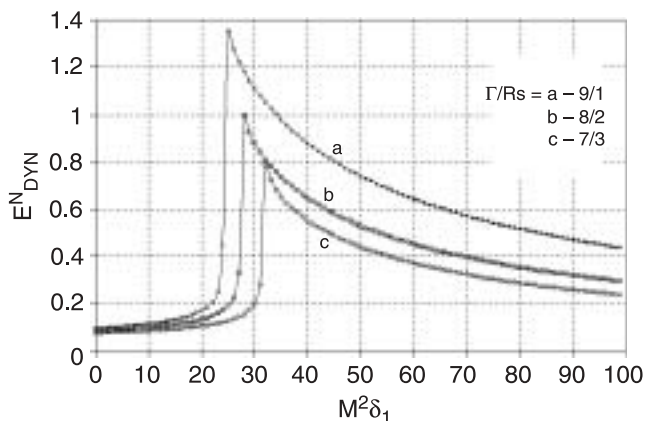


Fig. 6. Normalized energy emitted on dynamic losses of the laser cavity vs. $M^2\delta_1$ parameter for SA without ESA. $T_1 = 1$.

mines the necessity of using saturable absorbers characterized by higher absorption cross section or it forces us to make an artificial modification of $M^2\delta_1$ parameter by using the higher enlargements M of a generated laser beam.

The behaviour of a Q-switched laser with SA characterized by ESA was presented in Figs. 7 and 8. It is easy to observe, that excited state absorption phenomenon in SA negatively influences laser generation efficiency causing decrease in the energy emitted on static losses and simultaneously increasing the energy which saturates SA. The differences between E_{STAT}^N and E_{DYN}^N versus Γ/R_s ratio are higher than for SA without ESA.

From the diagrams presented above (depending on $M^2\delta_1$ parameter value), we can specify three different working regimes of a passive Q-switched laser:

- the case when $M^2\delta_1 \gg 1$. Then we deal with a well designed passively Q-switched laser. The laser medium is strongly saturated. For SA without ESA, the small amount of the energy stored in the laser cavity is destined for dynamic losses switching. Most of the energy stored is emitted on transmission and dissipative losses. However, as far as a laser with SA characterized by ESA is concerned, the energy saturating SA is constant versus $M^2\delta_1$ parameter value.

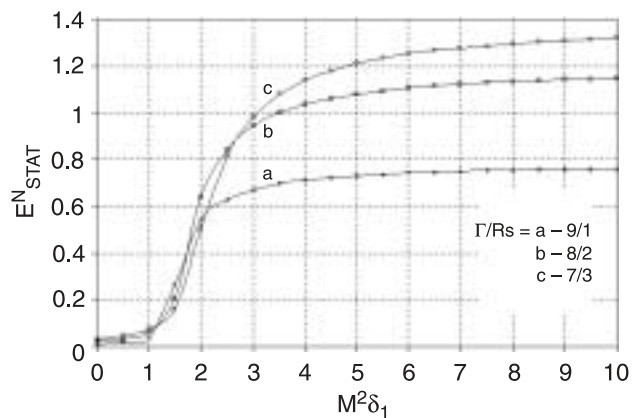


Fig. 7. Normalized energy emitted on static losses of the laser cavity vs. $M^2\delta_1$ parameter for SA with ESA. $T_1 = 1000$, $T_2 = 1$, $\delta = 0.2$.

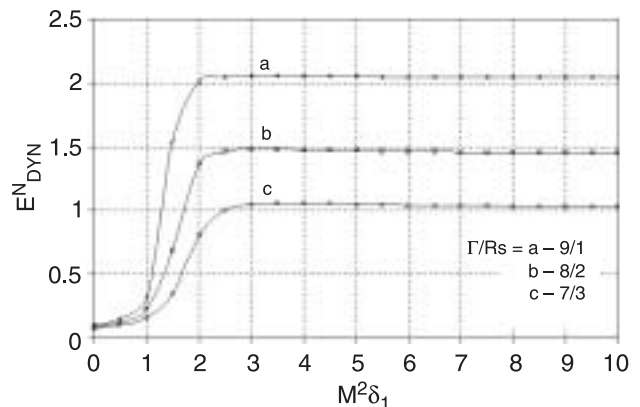


Fig. 8. Normalized energy emitted on static losses of the laser cavity vs. $M^2\delta_1$ parameter for SA with ESA. $T_1 = 1000$, $T_2 = 1$, $\delta = 0.2$.

- the case when $M^2\delta_1 < 1$. The gain in LM is weakly saturated and the energy generated is very small. In extreme case, when $M^2\delta_1 \rightarrow 0$ (we can interpret it as using an absorber with absorption cross section close to zero and characterized by some finite transmission resulting from absorbing centres concentration) our laser works in free running regime. The losses introduced by SA are not changeable during the generation and such an absorber cannot be called nonlinear.
- the case when $M^2\delta_1 > 1$ (where energy changes are the highest). In this range along with the increase of $M^2\delta_1$ value the gain saturation of LM builds up rapidly, especially for high values of Γ/R_s ratio value. It is caused by absorption saturation of a SA. There is an explicit maximum of energy switching the SA, whose location depends on Γ/R_s ratio. This range can be called ineffective Q-modulation.

It is not difficult to conclude from the analysis done so far, that for a laser with a SA exhibiting ESA as well as a laser with a SA characterized by the lack of ESA phenomenon the relations of the energy emitted on the static losses R_s change as a function of the ratio of the whole laser loss components. It points to the necessity of optimization of the laser transmission losses R_T depending on dissipative losses R_D and $M^2\delta_1$ parameter.

Figures 9 and 12 present dependences of normalized output laser energy as a function of Γ/R_s ratio. The dissipative losses were assumed at 1%, 5%, and 10% of initial gain. On the basis of the characteristic curves presented above we can point the optimum Γ/R_s ratio for which the output energy is maximum. This maximum is strongly dependent on dissipative losses level, which is obvious ($R_s = R_T + R_D$). The higher value of dissipative losses corresponds to lower laser output energy (Figs. 11 and 12) and the higher value of $M^2\delta_1$ corresponds to the higher output energy. Along with increase of $M^2\delta_1$, the maximum of output energy shifts towards the lower values of Γ/R_s ratio, and the level of this maximum increases. The optimal output energy is strongly limited especially from low values of Γ/R_s ratio direction. In this range, the slight change of this

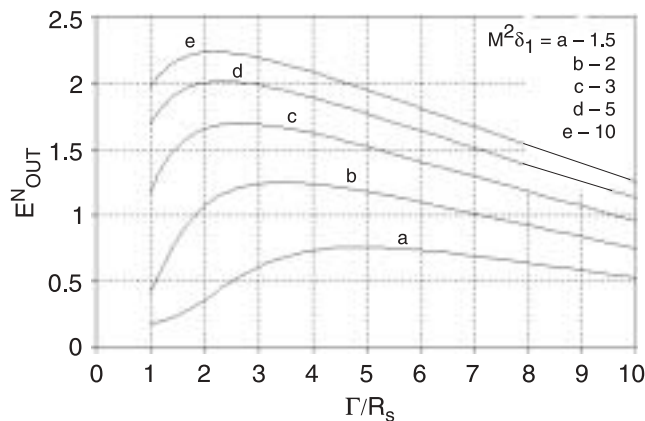


Fig. 9. Normalized output laser energy vs. Γ/R_s ratio for the laser with SA without ESA. Dissipative losses $R_D = 5\%$. $T_1 = 1000$.

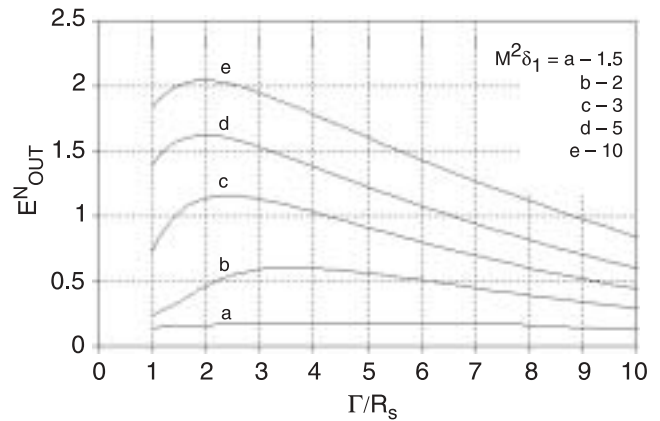


Fig. 10. Normalized output laser energy vs. Γ/R_s ratio for the laser with SA characterized by ESA. Dissipative losses $R_D = 5\%$. $T_1 = 1000$, $T_2 = 1$, $\delta = 0.2$.

ratio induces significant changes of output energy. This limitation occurs especially for higher values of dissipative losses (Fig. 12).

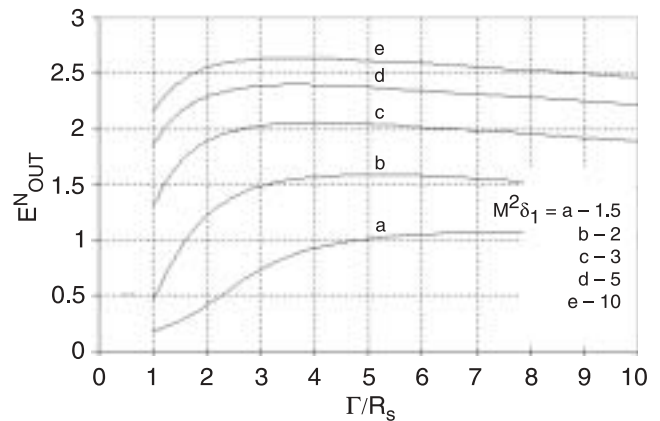


Fig. 11. Normalized output laser energy vs. Γ/R_s ratio for the laser with SA without ESA. Dissipative losses $R_D = 1\%$. $T_1 = 1000$.

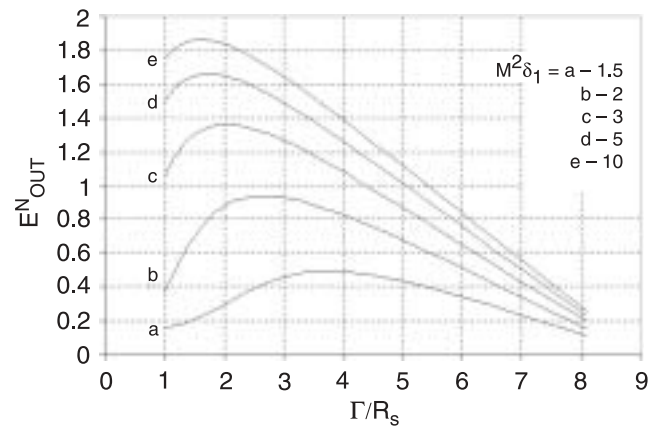


Fig. 12. Normalized output laser energy vs. Γ/R_s ratio for the laser with SA without ESA. Dissipative losses $R_D = 10\%$. $T_1 = 1000$.

Table 2. Compatibility comparison of simulation and experimental results.

Saturable absorber	Computer simulation		Experimental results	
	Pulse energy	Pulse width	Pulse energy	Pulse width
Cr ⁴⁺ :YAG	17.73 mJ	15 ns	16.6 mJ	14.4 ns
Cr ⁴⁺ :GSGG	3.26 mJ	30 ns	3.12 mJ	28.3 ns

6. Experimental verification of numerical analysis results

In order to confirm the correctness of the numerical analysis conducted in sec. 4, an experimental passively Q-switched laser set-up was elaborated. The $\phi 4$ -mm $\times 3.5$ ' Nd³⁺:YAG crystal was used as an active medium with both sides antireflection coated at 1060 nm. This crystal was pumped by a $\phi 4 \times 30$ mm xenon flash lamp and was located in a 92 cm-long plane-plane laser cavity. The rear reflector had nearly total reflection at 1064 nm, and another flat mirror acted as an output coupler with reflectivity of 15% (optimal value for Cr⁴⁺:YAG) and 70% (optimal value for Cr⁴⁺:GSGG). The pump light was focused by means of a diffusion elliptical cylinder reflector (LM 1520T C300S). In this set-up we applied a $\phi 2.25$ mm diaphragm forcing the laser to work in a fundamental transverse mode TEM₀₀. Cr⁴⁺:YAG and Cr⁴⁺:GSGG crystals, antireflection coated at 1064 nm, were used as passive switches. Applications of two different absorbers aimed to confirm the conclusions formulated earlier. Both Cr⁴⁺:YAG and Cr⁴⁺:GSGG crystals were characterized by excited state absorption and, what is the most important from experimental point of view, they are also characterized by different values of δ parameter. The Cr⁴⁺:YAG absorber was characterized by: $\sigma_a = 2.08 \times 10^{-18}$ cm², $l_{SA} = 0.55$ cm, initial transmission $T_0 = 17\%$, $\delta = 0.098$, $\delta_1 = 0.32$. However, Cr⁴⁺:GSGG crystal was characterized by: $\sigma_a = 1.5 \times 10^{-18}$ cm², $l_{SA} = 0.8$ cm, initial transmission $T_0 = 36\%$, $\delta = 0.19$, $\delta_1 = 2.3$. The experimental set-up worked with 1 Hz repetition rate. The Rj-7100 energy meter with Rjp-735 probe and the digital oscilloscope (2040 Tektronix) were used to measure the output energy and the pulse width of the laser pulse, respectively. It was necessary to compare the obtained measurement results with those achieved by applying the numerical calculations. This comparison is presented in Table 2.

All pulse characteristics, such as output energy and pulse duration were in very good agreement with those predicted theoretically. Thus, it allows us to assume that the numerical model proposed is correct and can be applied for different saturable absorbers both with and without ESA phenomenon.

7. Conclusions

In conclusion, the optimization of a passively Q-switched laser with saturable absorber characterized by ESA was considered. We developed a detailed analysis of the passively Q-switched lasers based on the normalized dimensionless rate equations considering: ESA and lifetimes of the SA as well as the magnification in the laser cavity. The following conclusions were drawn from the analysis presented above:

- efficient generation in a passively Q-switched laser takes place when a saturable absorber is characterized by the absence of ESA.
- in order to maximize the laser output energy, the saturable absorber should be characterized by long lifetime of its first excited state as well as high value of the ratio of ground state absorption cross section of a SA to emission cross section of a LM. It guarantees high saturation of a laser medium.
- ESA phenomenon decreases the laser generation efficiency. It results from multiple absorption transitions between excited states of a SA. The ESA phenomenon causes: the decrease in the energy emitted on static (dissipative and transmission) losses of a laser cavity, the increase in the energy level which is necessary to "switch" a saturable absorber, and the fall of laser medium gain saturation.
- the level of the energy emitted on all the laser cavity losses depends on the ratio of its particular components. This relation occurs especially in case of a SA characterized by ESA.

The theoretical and experimental results obtained are in very good agreement and thereby they are very useful in designing of such lasers.

References

1. W. Koechner, *Solid State Laser Engineering*, 5th edition, Springer-Verlag, Berlin, 2001.
2. L. Chen, S. Zhano, J. Zheng, Z. Cheng, and H. Chen, "Characteristics of a passively Q-switched Nd³⁺:NaY(WO₄)₂ laser with Cr⁴⁺:YAG saturable absorber", *Optics & Laser Technol.* **34**, 347–350 (2002).

3. J. Liu, J. Yang, and J. He, "High repetition rate passively Q-switched diode pumped Nd:YVO₄ laser", *Optics & Laser Technol.* **35**, 431–434 (2003).
4. J. Degnan, "Optimization of passively Q-switched lasers", *IEEE J. Quantum Electron.* **31**, 1890–1901 (1995).
5. X. Zhang, S. Zhao, Q. Wang, Q. Zhang, L. Sun, and S. Zhang, "Optimization of Cr⁴⁺-doped saturable – absorber Q-switched lasers", *IEEE J. Quantum Electron.* **33**, 2286–2294 (1997).
6. M.B. Camargo, R.D. Stultz, and M. Birnbaum, "Co²⁺:YSGG saturable absorber Q-switched for infrared erbium lasers", *Opt. Lett.* **20**, 339–341 (1995).
7. V.B. Sigacher, T.T. Basier, M.E. Doroshenko, V.V. Osiko, and A.G. Popashvili, "1.3 μm neodymium laser passively Q-switched with Nd²⁺:SrF₂ and V³⁺:YAG crystal and Raman shifting to eye-safe region", *Adv. Solid State Lasers OSA TOPS* **24**, 460–463 (1995).
8. Y.K. Kuo, M. Birnbaum, W. Chen, K. Yue, and M.F. Huang, "Passive Q-switching of the Tm, Cr:YAG 2 μm laser with a HLF solid-state saturable absorber", *Adv. Solid State Lasers OSA TOPS* **24**, 445–450 (1995).
9. U. Griebner and R. Koch, "Passively Q-switched Nd:glass fibre-bundle laser", *Electron. Lett.* **31**, 205–208 (1995).